

Co-published by Institute of Fluid-Flow Machinery Polish Academy of Sciences

Committee on Thermodynamics and Combustion

Polish Academy of Sciences

Copyright©2025 by the Authors under licence CC BY-NC-ND 4.0

http://www.imp.gda.pl/archives-of-thermodynamics/



Sustainable air conditioning with a focus on evaporative cooling and the Maisotsenko cycle

Jan Pokorný^{a*}, Paweł Madejski^b, Jan Fišer^a

^aFaculty of Mechanical Engineering, Department of Thermodynamics and Environmental Engineering, Brno University of Technology (BUT),

Technická 2896/2, Královo Pole, 61669, Brno, Czech Republic

^bFaculty of Mechanical Engineering and Robotics, Department of Power Systems and Environmental Protection Facilities,

AGH University of Science and Technology, al. Mickiewicza 30, 30-059 Kraków, Poland

*Corresponding author email: pokorny.j@fme.vutbr.cz

Received: 29.01.2025; revised: 05.05.2025; accepted: 27.05.2025

Abstract

Evaporative cooling can be an answer to the growing global demand for energy efficient and sustainable air conditioning. Direct evaporative cooling is the traditional method of cooling air to wet-bulb temperature. Indirect evaporative cooling uses heat exchangers with wet and dry channels to cool air indirectly, avoiding an increase in humidity. The Maisotsenko cycle is a dew point indirect evaporative cooling that allows air to be cooled below wet-bulb temperature using a heat and mass exchanger with a coupled wet and dry channel. It can be used as a stand-alone system, or as coupled with traditional refrigerant-based cooling systems, or as a heat recovery process to improve the efficiency in the power industry applications. A Python-based computational tool for simulating of 1D heat and mass transfer in the Maisotsenko cycle is presented here. It uses a spatially discretised differential equation solver and a psychrometric chart. The 1D model and experimental data from the study of Pakari were used as a reference for the initial testing. The comparison results are promising, suggesting a potential application in the design of sustainable cooling.

Keywords: Sustainability; Cooling; M-cycle; Python; 1D model

Vol. 46(2025), No. 2, 111-121; doi: 10.24425/ather.2025.154911

Cite this manuscript as: Pokorný, J., Madejski, P., & Fišer, J. (2025). Sustainable air conditioning with a focus on evaporative cooling and the Maisotsenko cycle. *Archives of Thermodynamics*, 46(2), 111–121.

1. Introduction

The challenges posed by climate change and rapid population growth, particularly in urbanizing regions, have intensified the demand for sustainable cooling technologies. Currently, India and China together account for 35% of the global population, which is approximately 8.2 billion people [1], as illustrated by the population density map in Fig. 1. According to United Nations population projections [2], the global population is expected to reach 10 billion by 2060. The combination of population growth and global warming presents challenges for governments, requiring proactive measures to address both the causes and consequences of these issues. Tackling these challenges de-

mands innovative solutions and a shift toward more sustainable technologies, especially by rethinking energy use and emission production. "Under the Paris Agreement of 2015, every five years countries review their progress in limiting greenhouse gas emissions. The key aim is to curb the rise in global average near-surface temperature, holding it to well below 2°C above pre-industrial levels, and to pursue efforts to limit the increase to 1.5°C" [3]. In 2018 the Intergovernmental Panel on Climate Change (IPCC) published the report Global Warming of 1.5 [4], which emphasized the need for global action to halve emissions by 2030 and achieve net-zero emissions by 2050. It was projected that the 1.5°C limit could be reached between 2030 and 2052.

Nomenclature

- specific heat capacity of air, J/(kg·K)

h – convective heat transfer coefficient, W/(m²·K)

 h_m – mass transfer coefficient, m/s

 h_{fg} – latent heat of vaporization of water, J/kg

- height of the channel, m

– thermal conductivity, $W/(m \cdot K)$ k

L- length of the channel, m

- mass flow rate, kg/s

- barometric pressure, kPa p

- time, s

T- temperature, K

- heat transfer coefficient, W/(m²⋅K)

- axial distance along the channel, m

Greek symbols

- thickness, m

- effectiveness, %

density, kg/m³

- relative humidity, %

- specific humidity, kg/kg_{da}

Subscripts and Superscripts

[0] – start point of vector (Python)

[-1] – end point of vector (Python)

dry air

- dry channel air

dp – dew point

in - inlet

pl - plastic - wet channel air

wf - saturated air at water film

wb - wet-bulb

m - mass out - outlet

pa – paper

Abbreviations and Acronyms

- air conditioning

BVP - boundary value problem

C3S - Copernicus climate change service

CFD - computational fluid dynamics

COP - coefficient of performance

DEC - direct evaporative cooling

EC. evaporative cooling

ECMWF- European Centre for Medium-Range Weather Forecasts

FDM - finite difference method

GWP - global warming potential

HMX - heat and mass exchanger

- heat exchanger

HVAC - heating, ventilation, air conditioning

- indirect evaporative cooling

IPCC - Intergovernmental Panel on Climate Change

- initial value problem

M-cycle- Maisotsenko cycle

ODEs – ordinary differential equations

PDEs – partial differential equations

- technology readiness levels

VCC vapour compression cycle

According to the recent data (November 2024) from Copernicus Climate Change Service (C3S) [5], the Earth reached this 1.5°C limit already in 2024 with the average near-surface temperature of the Earth 15°C. The prediction [6] expected that in the year 2060, there would be an increase of 2°C or even more than in the pre-industrial period in the pessimistic case scenario, which seems to be more probable today than in 2016, see Fig. 2.

The sustainability of technologies related to climate change is more important than ever, leading to a rethinking of strategies for cooling and air conditioning (AC) systems. Traditional cooling technologies, such as vapour compression cycles (VCC), rely heavily on refrigerants that significantly contribute to the greenhouse effect. Due to stricter legislation, refrigerants with high Global Warming Potential (GWP) are being phased out. The European Commission's study on cooling technologies under the revised Renewable Energy Directive underscores the importance of shifting towards renewable and energy-efficient cooling methods, away from high GWP refrigerants toward more sustainable alternatives. In the [7], the review of cooling technologies, the environmental impacts, efficiencies, and Technology Readiness Levels (TRL) are listed.

Generally, cooling systems can be based on electrical (e.g. thermoelectric Peltier modules), mechanical (e.g. VCC), acoustic, magnetic (e.g. magnetocaloric), chemical (e.g. desiccant systems, heat of reaction), hydraulic (e.g. potential energy use), thermal (e.g. absorption and adsorption, transcritical thermal compression heat pumps), and natural physical phenomena (e.g. natural convection, evaporative cooling systems). A promising alternative to VCC in some applications are



Fig. 1. Population density: processed from sources [8,9].

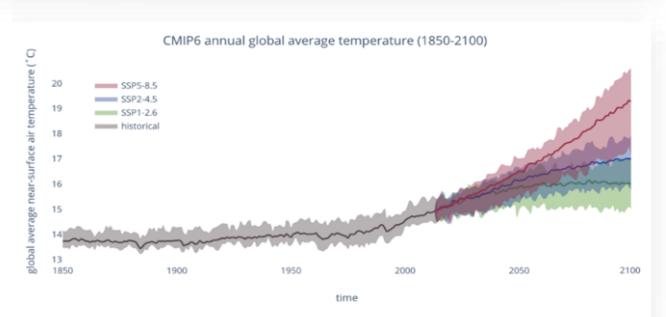


Fig. 2. Global mean temperature between 1850 and 2100. Projection from [6] published in 2016. The grey shows the past and the coloured areas show projections of future temperature based on greenhouse gas emission scenarios (red is pessimistic, blue is realistic and green is optimistic). Credit: C3S, ECMWF.

evaporative cooling (EC) systems, which generally allow for reaching the wet-bulb temperature and in this range can achieve interesting values of coefficient of performance (COP) at the expense of water consumption. By [10], the evaporative cooling can reach COP values (15-20), which are very good values in comparison with VCC (2-4), absorption/adsorption (0.6-1.2) or thermoelectric cooling by the Peltier effect (0.2–1.2). The reason for the good COP is that unlike in VCC where a compressor is used, in evaporative cooling (EC), only power supply of a fan or a water pump is needed to provide the required cooling effect, primarily through water consumption. However, the limitation of standard EC is that the cooling requirements must remain above the wet bulb temperature. The EC system can be used as a stand-alone system, or as coupled with traditional refrigerantbased cooling systems, or as a heat recovery process to improve the efficiency in the power industry applications such as turbines [11]. An example of the coupled EC and VCC system is an evaporative condenser to lower system condensing temperatures and reduce the compressor workload. A more advanced solution is the so-called M-condenser [12].

This paper focuses on EC systems for heating, ventilation, and air conditioning (HVAC) applications. The challenges related to the demand for sustainable cooling technologies have already been outlined.

The subsequent part of the introduction presents a brief literature review of evaporative cooling, including Maisotsenko cycle (M-cycle) technology; discusses the potential of EC and our research objectives, emphasizing the advanced materials, innovative structures, and system integration to enhance the efficiency of cooling technologies, especially EC systems.

Finally, the main contribution of this study is the development of a Python-based one-dimensional model of heat and mass transfer for M-cycle calculations inspired by Pakari's study [13]. His 1D model simulated in COMSOL and his experimental data were used as a reference for presented benchmark tests.

1.1. Evaporative cooling

EC can be understood as a physical process which uses the transition of liquid water to water vapour to the cooldown of the wetted surface based on the principle of adiabatic cooling. This phenomenon occurs naturally in trees and plants, which regulate water loss through micropores in their leaves; similarly, humans regulate water loss through sweat glands and pores in the skin. By the long-term adaption, they adjusted to manage control of the water loss to survive in different climatic zones. Human civilisation has used EC as a fundamental method for temperature control for centuries, utilized in various forms across different cultures – Mashrabiya architecture for cooling of buildings [14], terracotta pots for beverage and food storage etc. These traditional techniques are still widely used because of their simplicity even in the modern design of buildings. They can be combined with new architectural strategies like optimizing building orientation, incorporating advanced natural ventilation systems, integrating plants on building facades for shading and evapotranspiration, or new solar cooling technologies [15], etc. These approaches significantly contribute to lower thermal loads and reduce energy consumption of HVAC systems. The evaporative cooling can be categorized into [14]:

- Direct Evaporative Cooling (DEC) active, passive,
- Indirect Evaporative Cooling (IEC) wet bulb, sub-wet bulb (M-cycle),
- Combined Indirect/ Direct Evaporative Cooling (IDEC) multi stages.

Direct Evaporative Cooling (DEC) is the traditional method of cooling air to wet bulb temperature, which can be active or passive. Active cooling typically uses a fan or water pump for increasing of efficiency. Passive cooling is naturally driven with no power consumption. DEC systems are particularly effective in dry climates, where high temperatures and low air humidity levels enhance the cooling effect. However, in humid regions, these systems may increase moisture levels, which can reduce indoor thermal comfort [16].

Indirect Evaporative Cooling (IEC) systems cool air indirectly through a heat exchanger (HX), avoiding an increase of humidity in the produced air. This makes them suitable for a broader range of climatic conditions and applications where traditional DEC systems might not be suitable [17]. HX can have different setups of wet and dry channels (counterflow, crossflow, etc.) based on the specific application. The M-cycle is a dew point or so-called sub-wet bulb IEC that allows air to be cooled below the wet bulb temperature using a heat and mass exchanger (HMX) with a coupled wet and dry channel. Mahmood et al. [16] provided a comprehensive overview of dew point evaporative cooling.

To enhance efficiency, combined systems integrating IEC and DEC, also referred to as two-stage or multi-stage evaporative cooling systems, can be utilized. In a two-stage system, the air is initially cooled through indirect adiabatic cooling before undergoing direct adiabatic cooling in the subsequent stage. These combined systems can achieve higher cooling efficiencies while maintaining better control over humidity levels. This makes them particularly well-suited for applications where precise environmental control is required, such as in food storage and specific industrial processes. More information on combined systems can be found in [18].

The efficiency of general EC systems is typically assessed by evaluating their wet-bulb effectiveness, Eq. (1), which measures how effectively the system cools air relative to the wet-bulb temperature. The wet-bulb effectiveness ε_{wb} of the cooling system is defined, according to Pescod [19]. For the M-cycles, it also makes sense to evaluate the dew point effectiveness ε_{dp} , which is defined by Eq. (2) to express how effectively the system cools air relative to the dew point temperature [16]:

$$\varepsilon_{wb} = \frac{T_{d,in} - T_{d,out}}{T_{d,in} - T_{d,in,wb}}, \qquad (1)$$

$$\varepsilon_{dp} = \frac{T_{d,in} - T_{d,out}}{T_{d,in} - T_{d,in,dp}},$$
(2)

where $T_{d,in}$ is the dry channel inlet air temperature, $T_{d,out}$ is the produced air temperature at the dry channel outlet, $T_{d,in,wb}$ is the wet-bulb temperature of the air entering the dry channel and $T_{d,in,dp}$ is the corresponding dew-point temperature.

The theoretical limit of 100% effectiveness for DEC and IEC processes is the wet-bulb temperature, whereas for the M-cycle, it is the dew point temperature. The typical wet-bulb effectiveness of the DEC system ranges from 70% to 95%, depending on the air temperature and relative humidity, as well as other factors such as airflow rate and system design. The IEC system has typically an efficiency between 60–85%. M-cycles, under very specific conditions, can achieve wet-bulb effectiveness up to 180%, as reported by Mammod et al. [16]. However, typical values range from 110% to 120%, according to Pakari and Ghani [13], and 112%, as reported by Jradi and Riffat [20]. These values correspond to dew point effectiveness of 70% to 80%.

To increase system cooling efficiency in hot humid conditions it is possible to use some desiccation technologies to reduce the air humidity at the inlet to the cooling systems. Desiccants are hygroscopic materials which are able to reduce water content from humid air in a natural way. Silica gel, calcium chloride or similar absorption/adsorption materials are typically used. The list of studies related to this topic was published in [21–27]. The sustainability of the cooling system can be even improved with the solar driven ejector [28], water pump and fan to reduce power consumption from the electricity distribution grid to zero. So, these solar powered systems have zero CO₂ emission during their operation. Ge et al. [29] reviewed solar powered rotary desiccant wheel coolant systems, and Pacak and Worek [30], Pandelidis and Anisimow [31] investigated the application of the M-cycle for these systems.

Costelloe and Finn [17] stated that: "Desiccant AC has two main disadvantages. One is direct evaporative cooling, by which moisture is added to the air. In DEC, the limitation is the wetbulb temperature (wet-bulb effectiveness), which is almost impossible to reach by typical direct cooling. Another disadvantage is the size of the system. Both the rotary heat exchanger and the spraying chamber need significant volume".

Related to the sustainability in some regions is easy to supply salt water rather than fresh water even with a slightly lower cooling performance [32]. The wet-bulb and dew point temperate lowered with a lower barometric pressure. This is typically used to improve the efficiency of refrigeration as vacuum cooling of food [33], which is a rapid cooling technique for any porous product that has free water and uses the principle of evaporative cooling. Additionally, membrane-based vacuum air dehumidification [34] can provide a solution for building air conditioning in combination with hollow fibre membranes [35].

Another practical factor which influences the efficiency of evaporative cooling systems are pressure losses and the maintenance to avoid clogging of the evaporative system (pad) by pollutants or water stone, etc. Evaporative coolers with a sprayed bed (wet channel) differ from each other in terms of construction and the used material. The simplest construction is a free-bed evaporative cooler, which can be made of a simple material, e.g. wood chips, sponge, non-woven fabric, or cellulose pad (Fig. 3). Water is pumped and poured onto the bed, along which it trickles and reaches the lower tray, where it is pumped again and supplemented with the evaporated amount. The issues related to the sustainability of usage of different types of natural or synthetic materials pads are discussed in a literature review

of Kapilan et al. [18]. For AC applications, DEC limits the technology by increasing the outcoming humidity, which is good for some agriculture applications such as chicken farms, agriculture product storage (fruit, vegetable) or AC of greenhouses. For building applications [20,37–41], IEC provides better control about humidity at the outlet and is also safer regarding the health risks associated with mould formation in the working channels, which can spread more easily in DEC.

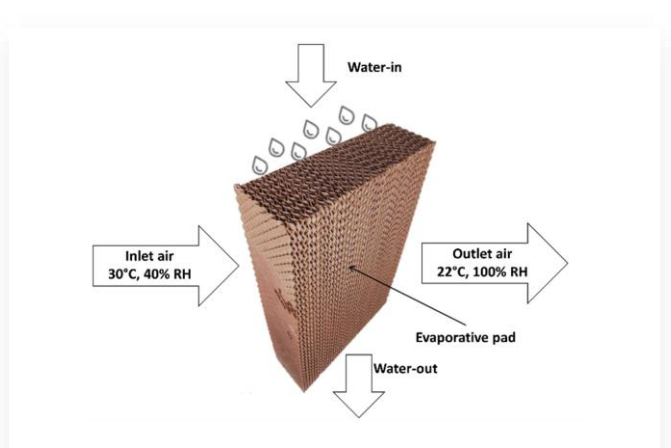
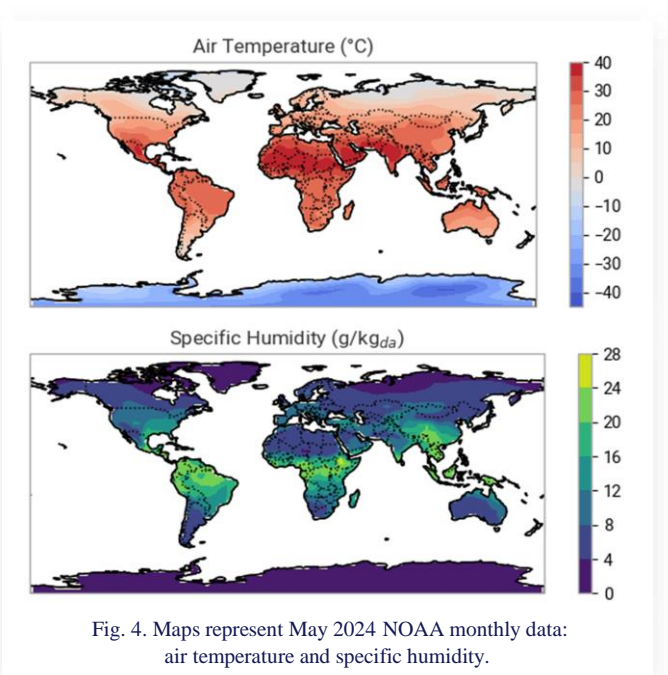


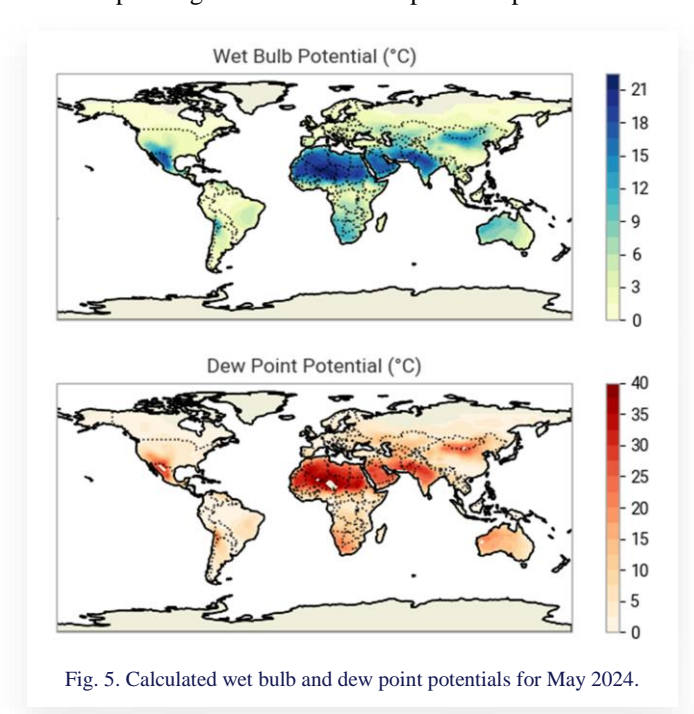
Fig. 3. Cellulose pad for direct evaporative cooling, cheap and efficient solution for cooling greenhouses, or even rooms in which higher outlet humidity does not cause problems. Source [36].

1.2. Potential of evaporative cooling

Another important aspect is determining where evaporative cooling systems are most effective, which depends largely on the Earth's climatic conditions, influenced by seasonal and time variations. The maps in Fig. 4 illustrate the average climatic conditions for May 2024, which is considered a warm month for the Northern Hemisphere, though not the hottest, which is July. The first map shows the average temperature, while the second map represents specific humidity. These maps are based on the datasets: <code>pressure/air.mon.mean.nc</code>, <code>shum.mon.mean.nc</code> from downloads.psl.noaa.gov/Datasets/ncep.reanalysis/Monthlies.



The dew-point and wet-bulb potential maps (Fig. 5) were calculated and visualised by EMCWF Python tool "earthkit". A similar map can be found in publications related to the storage of vegetables and fruits [42]. The potential calculations take into account the difference between average climatic conditions and the corresponding wet-bulb and dew-point temperatures.



In these visualizations, if the wet-bulb or dew point temperature falls below 0°C, it is set to 0°C, without considering the effects of sublimation. These maps indicate that the potential for EC is the highest in regions such as India, northern China, the eastern United States, and the Middle East and North Africa. However, due to ongoing global warming, this potential is also increasing in southern and central European countries. Notably, the difference between dew-point and wet-bulb potentials highlights where the M-cycle could be most beneficial.

1.3. Maisotsenko cycle

Modern EC technologies are still evolving significantly [43,44] and in this study, we focused specifically on sub-wet bulb evaporative cooling using the M-cycle. The M-cycle represents an IEC method that enables cooling below the wet-bulb temperature by utilizing a configuration of alternating wet and dry channels within a heat and mass exchanger. The M-cycle's ability to achieve such low temperatures without the need for refrigeration makes it an attractive option for both HVAC applications and power engineering. Its versatility extends to hybrid systems, where it can be integrated with traditional refrigerant-based systems (VCC). This combination maintains high cooling capacity while reducing the environmental impact associated with conventional refrigerants.

According to Taler et al. [45], there are still challenges for research in the field of IEC and M-cycles such as: improvement of water and air distribution inside channels; developing of new materials dedicated for IEC for greater heat and mass transfer, lower pressures drops and better applicability; looking for novel

solutions and connection with IEC to increase the efficiency of the systems. For example, applying a novel bare tube plastic heat exchanger to desiccant M-cycle air conditioning. Kang et al. [46] already published the numerical optimisation of such a kind of bare tube plastic heat exchanger.

1.4. Advanced materials and system integration

Our research, conducted within the framework of the Brno University of Technology (BUT), project Mechanical Engineering of Biological and Bio-inspired Systems (MEBioSys) tries to transfer bio-inspired solutions from the long-term evolution to innovative technical solutions. Our main goal is to develop and optimize innovative evaporative cooling systems, exploring the use of various materials and structures such as smart membranes, which can be used in bio-inspired evaporative pads.

In the EC system, the most important component is the wetted pad and techniques how the material of the pad absorbs and reveals water. Recent studies, including those by Mumtaz et al. [22] and Kapilan et al. [18] highlight the potential of natural fibres and materials, emphasizing their availability and the reuse of natural resources to enhance system efficiency. Understanding natural processes and materials is crucial for identifying key parameters in the design of industrial heat exchangers, such as those manufactured using advanced methods like 3D printing with additive lattice structures [47]. Strategies for water sprays and membrane designs with controlled interface layers for optimal water evaporation and vapour condensation remain also highly relevant for ongoing areas of research [48-51]. The literature review highlighted the potential of innovative materials, such as membrane-based and bio-inspired evaporative pads, to enhance the cooling system efficiency.

2. Materials and methods

This paper aims to provide Python-based computational tools for simulation and visualisation of M-cycles. The computational tool utilizes a discretized approach to model the heat exchanger, dividing the process into small sections to solve the governing equations for heat and mass transfer iteratively. This approach allows for detailed analysis of the thermal performance across different sections of the M-cycle. This paper presents the first step to reproduce the established and validated model of Pakari and Ghani [13], and compare results to ensure the validity of our Python model. This iterative process of refinement and validation is crucial for further developing a reliable computational tool. The hypothesis was given that this kind of model is able to support the design of the M-cycle, and that the model can reproduce the data from the Pakari study. The next steps will involve validating our 1D model using our own 3D-printed complex geometry. Additionally, strategies for water spraying and the use of advanced materials will be considered in the subsequent phases of our research.

2.1. Computational tool development

To support the design and optimization of EC and M-Cycle systems, a 0D/1D computational tool has been developed in Python. This tool is designed for psychrometric calculations and

simulating the 1D heat and mass transfer during evaporation. The CoolProp library is used as the dataset of humid air properties. The developed Python library includes modules for calculating humid air properties using Coolprop, visualizing data on a psychrometric chart, Mollier diagram, and implementing a discretized model for heat and mass transfer calculations. For the development, the Python 3.10 and Spyder 5.5 were used. The main code requirements of libraries are: "CoolProp, matplotlib, numpy, openpyxl, plotly, pandas, scipy". These libraries allow us to create datasets compatible with Excel and interactive charts, and provide a support for the calculation of humid air properties and numerical solution for the differential equations.

2.2. Pakari's study

The experimental setup is described in the Pakari study and the details about definition of each term of the system of differential equations can be found in [13]. In this paper, we focused just on the description of the developed 1D M-cycle model in Python, which is designed to solve the heat and mass transfer in HMX including evaporation. The scheme of simulated M-cycle is depicted in Fig. 6 and it corresponds to the Pakari scheme of his experimental test bench.

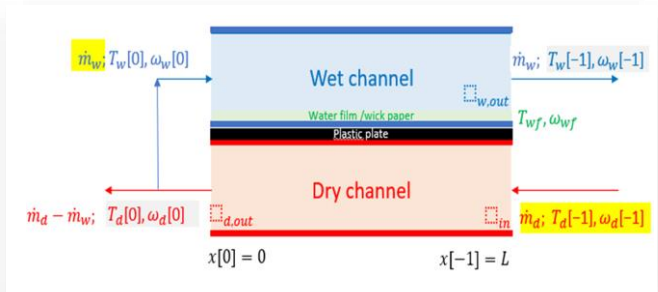


Fig. 6. Scheme of the one channel pair: dry and wet.

For the simulation, the exact dimensions of Pakari's M-cycle HMX are used. The physical constants such as the conductivity of materials (paper, plastic wall) are the same, and also the same assumption are made about flow characteristics such as the Nusselt number, etc. The Pakari HMX consists of 50 pairs of dry and wet channels in counter-current arrangement with the following geometrical parameters: channel length L=0.5 m; channel height H=0.3 m; heat exchanger width 0.22 m; dry channel width 2 mm; wet channel width 2 mm; plastic plate thickness $\delta_{pl}=0.2$ mm; paper thickness $\delta_{pa}=0.15$ mm.

Pakari experimentally investigated 15 different test cases, see Table 1, showing all input values of temperature and humidity at the dry channel inlet (T_{in}, ω_{in}) and mass flows in the dry (m_d) and wet channel (m_w) . These inputs to the 1D M-cycle model are highlighted in yellow in Fig. 6 and in Table 1 and denoted by subscript in). The mass flows m_d and m_w are the sum of 50 pairs of the dry and wet channels. The mass flow difference $m_d - m_w$ is the air produced at the dry channel outlet. The primary focus of Pakari was on the produced air at the outlet of the dry channel $(T_{d,out}, \omega_{d,out})$ referred to in the numerical scheme as $(T_d[0], \omega_d[0])$. However, he also evaluated by his model the working air at the outlet of the wet channel $(T_{w,out}, \omega_{w,out})$ referred to in the numerical scheme as $(T_w[-1], \omega_w[-1])$ by his 1D and 3D model. In this study, we use for verification the ex-

perimental values and also the values from his 1D model (these parameters are highlighted in grey in Fig. 6).

Test No.	<i>T</i> _{in} (°C)	φ _{in} (%)	ω_{in} (g/kg _{da})	m_d (kg/s)	m_w (kg/s)	
1	29.2	43.2	10.9	0.0465	0.0154	
2	30.1	43.0	8.8	0.0468	0.0153	
3	30.2	30.0	8.3	0.0643	0.0193	
4	30.3	31.0	8.1	0.0493	0.0157	
5	30.5	34.0	9.1	0.0694	0.0256	
6	30.5	38.0	7.7	0.0450	0.0108	
7	35.1	28.0	9.9	0.0429	0.0157	
8	35.1	35.0	11.7	0.0504	0.0165	
<u>9</u>	35.2	43.0	10.7	0.0517	0.0167	
10	39.2	42.0	11.5	0.0655	0.0246	
11	40.2	29.0	11.3	0.0643	0.0143	

10.6

11.4

10.8

9.8

0.0643

0.0643

0.0525

0.0435

Table 1. Pakari's measured test data used as input for model verification.

2.3. Python model of the Maisotsenko cycle

22.0

22.0

17.0

17.0

43.9

43.9

44.2

44.2

12

13

14

15

The Python 1D model consists of the following set of differential equations describing heat and mass transfer in the M-cycle, see Eqs. (3) to (6):

- energy conservation in the dry channel (subscript *d*):

$$\rho_d c_d \frac{\partial T_d}{\partial t} + \dot{m_d} c_d \frac{\partial T_d}{\partial x} = UH(T_{wf} - T_d), \tag{3}$$

0.0143

0.0155

0.0252

0.0147

- energy conservation in the wet channel (subscript w):

$$\rho_w C_w \frac{\partial T_w}{\partial t} + m_w C_w \frac{\partial T_w}{\partial r} = h_w H (T_{wf} - T_w), \tag{4}$$

moisture conservation in the wet channel:

$$\rho_{w} \frac{\partial \omega_{w}}{\partial t} + \dot{m_{w}} \frac{\partial \omega_{w}}{\partial x} = h_{m} \rho_{a} H (\omega_{wf} - \omega_{w}), \tag{5}$$

energy conservation at the water film (subscript wf):

$$\rho_w C_{wf} \frac{\partial T_{wf}}{\partial t} + h_w H (T_w - T_{wf}) + UH (T_d - T_{wf}) +$$

$$+ h_m \rho_a h_{fg} (\omega_w - \omega_{wf}) + kHL \frac{\partial^2 T_{wf}}{\partial x^2} = 0,$$
(6)

where ρ is the density, c – specific heat capacity, T is the temperature, ω – specific humidity, H is the height of the channel, x – spatial domain, t – time domain, and h is the convective heat transfer coefficient. Remark: ω_{wf} is saturated humid air in equilibrium with the water film and thus can be evaluated as humid air in the psychrometric chart. The value U includes the value h_d and the effect of thermal resistance of walls (plastic + paper)

$$U = 1/(1/h_d + \delta_{pl}/k_{pl} + \delta_{pa}/k_{pa}). \tag{7}$$

For the proposed model, similar assumptions were made by Pakari that HMX is insulated and there is no heat transfer to the ambience through the walls. Only temperature variations in the *x*-axis are considered. The fluid (humid air) is incompressible and viscous dissipation is negligible. The flow in the channels is laminar and fully developed, steady with a constant mass flow, heat and mass transfer coefficients. And there is no heat accumulation in the wicked paper or plastic wall. The time derivatives are proposed to simulate the dynamic behaviour of the system reacting to the varying conditions at the dry channel inlet. However, the unsteady model which is able to deal with these time terms is not yet finished and it is still under development. In this paper, only steady model results will be presented.

2.4. Discretisation and boundary conditions

The proposed set of partial differential equations (PDEs) was suggested to be solved using the Crank-Nicholson scheme for unsteady-state conditions. In this paper, we present only the steady-state solution, where the governing equations are simplified to a set of ordinary differential equations (ODEs) by setting all time derivatives to zero as Pakari did in his 1D model solved by COMSOL. The numerical solution of the resulting two-point boundary value problem (BVP) [52] is solved using the shooting method with a forward finite difference scheme for spatial discretization of N = 1000 elements. A finer discretisation improves the accuracy of this method while keeping the computation time within seconds. The code is designed to solve the system of ODEs for these variables:

- Temperatures: T_d (dry channel), T_w (wet channel), T_{wf} (water film),
- Specific humidity (humidity ratios): ω_d (dry channel), ω_w (wet channel), ω_{wf} (at the water film interface).

And these boundary conditions:

- Dirichlet boundary for T_d and ω_d at x = L (right side of the dry channel) T_d [-1] = T_{in} ; ω_d [-1] = ω_{in} , where T_{in} , ω_{in} are input values defined in Table 2,
- Neumann boundary condition (no heat flux) at x = L for water film $dT_{wf}[-1] = 0$ and at x = 0 $dT_{wf}[0] = 0$,

Table 2. Results of 1D Python model for 15 test cases (TC). $\varphi_{w,out}$ and $\varphi_{wf,out}$ were always 100 %.

тс	<i>T</i> _{in} (°C)	φ _{in} (%)	$T_{d,out}$ (°C)	φ _{d,out} (%)	T _{w,out} (°C)	T _{wf,out} (°C)	€ _{wb} (%)	ε _{dp} (%)
1	29.2	43.2	19.3	77.7	25.4	26.2	107.9	71.5
2	30.1	43.0	15.5	72.9	23.3	24.8	121.4	75.3
3	30.2	30.0	20.4	55.5	26.7	27.4	82.3	51.4
4	30.3	31.0	16.9	67.3	24.4	25.7	110.7	68.9
5	30.5	34.0	19.3	64.9	24.1	25.5	96.7	61.7
6	30.5	38.0	22.6	53.0	28.3	28.7	66.3	42.5
7	35.1	28.0	24.4	90.2	28.5	29.3	112.5	82.6
8	35.1	35.0	18.9	72.3	28.0	29.4	115.4	76.2
<u>9</u>	35.2	43.0	21.5	72.5	30.1	31.3	109.2	74.9
10	39.2	42.0	18.5	69.0	29.4	31.0	117.5	77.3
11	40.2	29.0	25.5	72.7	30.9	32.5	101.9	73.8
12	43.9	22.0	19.7	64.9	28.3	31.0	115.5	76.9
13	43.9	22.0	22.7	65.3	34.0	35.6	109.1	75.7
14	44.2	17.0	25.2	71.2	31.7	33.8	106.7	77.3
15	44.2	17.0	20.8	63.8	33.1	34.9	113.6	76.8

• Coupled conditions for the wet and dry channel at x = 0 (left side of the dry channel) $T_w[0] = T_d[0]$ and $\omega_w[0] = \omega_d[0]$.

The shooting method solves the boundary value problem (BVP) by first converting it into an initial value problem (IVP). The method uses an initial guessed condition at x=0 for the unknown temperature $T_d[0]$ and ω_{in} . Since no change in specific humidity occurs within the dry channel, $\omega_d[0] = \omega_{in}$. For this initial guess, the solver based on the forward finite difference method provides an initial numerical solution, which is compared to the Dirichlet boundary condition at x=L (dry channel inlet). The solver is run iteratively to adjust the guess until the solution of dry channel temperature matches the boundary condition with an error lower than the given tolerance of 0.01° C. So when the condition $|T_d[-1] - T_{in}[-1]| < 0.01$ is satisfied then the final solution is given. This approach ensures consistency in handling the coupled heat and mass transfer processes across the dry channel, wet channel, and water film.

The proposed iterative procedure allows us to deal with the coupling of the wet and dry channel at x = 0, which is a key factor for the proper simulation of the M-cycle with countercurrent configuration.

3. Results

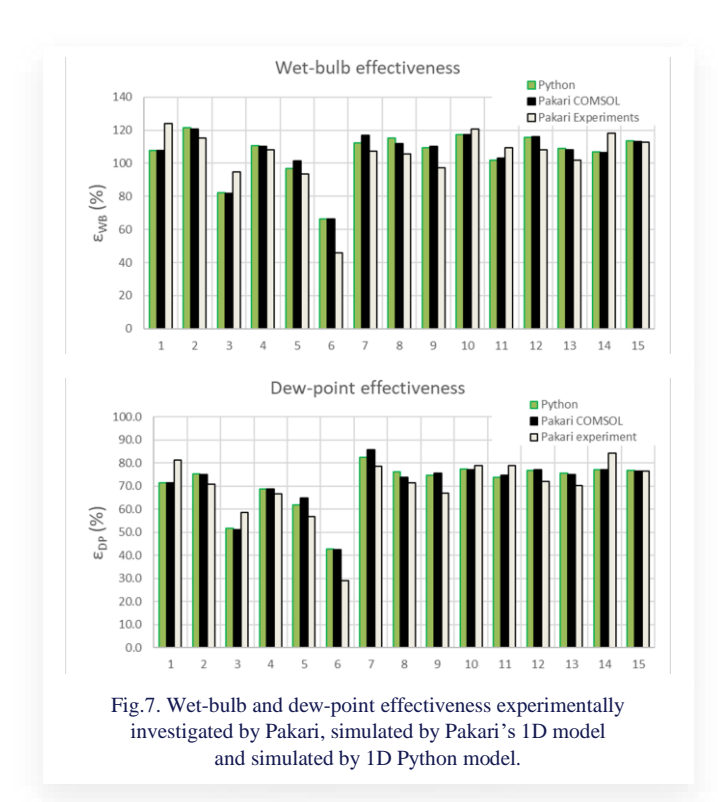
Simulations using the Python 1D model were performed for all 15 test cases from Table 1 to calculate the outlet dry and wet channel temperatures, humidity, and effectiveness. The results closely align with Pakari's experimental and simulation data.

3.1. Verification of the model on Pakari's data

The aim of this paper was to verify our Python model based on Pakari's experimental data and his 1D model. This chapter brings a summary of all simulated test cases. Table 2 presents the main results of the Python 1D M-cycle model for all test cases. The key outputs of the model are provided from the fourth column onward. Test case number 9 is underlined and highlighted because additional verification data were available for this test, see Chapter 3.2.

The verification of the simulated effectiveness is shown in Fig. 7, which compares the wet-bulb effectiveness as investigated experimentally by Pakari, simulated by Pakari's 1D model, and simulated by the Python 1D model. Additionally, these values are recalculated for the dew point effectiveness. Both calculated values of effectiveness are in good agreement with the results simulated in COMSOL by Pakari and also with experimental values.

The final verification is depicted in Fig. 8, where the outlet dry channel temperatures of the produced air are plotted and compared with Pakari's 1D model. Tolerance lines of 10% are highlighted, indicating that all test cases fall within this range, with the Python and Pakari models closely aligned. Ideally, the simulated results should lie on the diagonal of this chart to match Pakari's experimental data. Test cases 4 and 15 were closest to this ideal fit, while test case 6 was the furthest. Uncertainties during measurement and the estimation of some channel parameters should also be considered, meaning an ideal fit cannot be



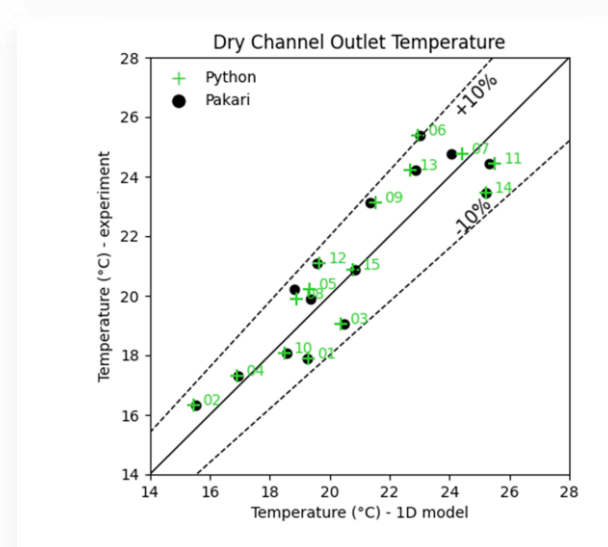


Fig. 8. Air temperatures produced at the outlet from the dry channel. The horizontal axis is from 1D model of Pakari and Python. The vertical axis are the corresponding measured data. The best agreement between simulation and measurement lies on the diagonal line of the

expected for all test cases. Still, the achieved results are very good, and the agreement between Pakari's and the Python simulation is particularly strong, indicating that the Python code verification was successful for all 15 test cases.

3.2. Verification of test case 9

Test Case 9 is highlighted in this section because it was published in the Pakari study with a more detailed analysis. For this test case, Pakari provided the resulting temperature profiles. Figure 9 compares the simulated temperature profiles with Pakari's results. Specific humidity data from the Pakari study were not available, so only simulated humidity profiles are presented. It can be observed that the water film has a higher temperature than

the wet channel, which aligns with the fact that heat transfer between the wet and dry channels is mediated by the water film separating them.

Other test cases do not have these spatial data available. However, the data come from the 1D Pakari's model, not the experiment, so the comparison of these profiles is just our Python model (line) versus Pakari's model (dots). The continuous lines represent 1000 discretised points by our model and the dots do not correspond to the discretisation used by Pakari (100 points). These dots just represent the shape of the resulting profiles and are used to clearly distinguish between both models. The dry channel has a red colour, the wet channel has a blue colour, and the water film is green. The temperatures and specific humidity profiles correspond to the visualisations in the psychrometric chart (Fig. 10) and in the Mollier chart (Fig. 11).

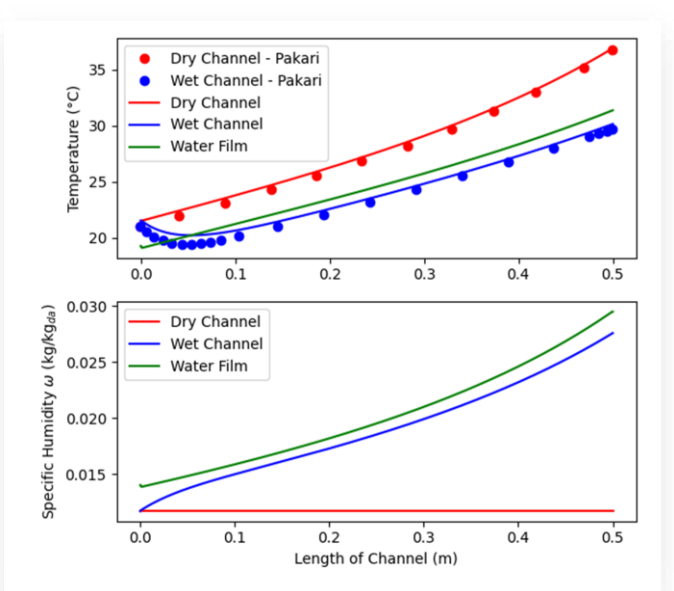
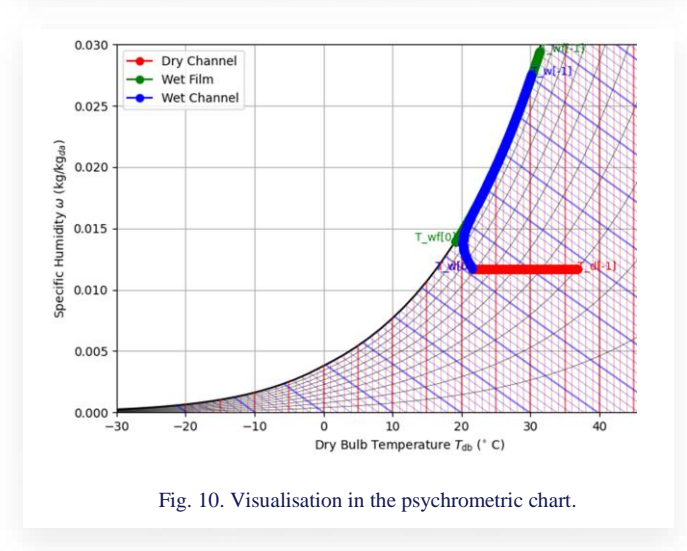


Fig. 9. Temperature and specific humidity profiles for the dry and wet channel and water film: Python model (lines) vs. Pakari's model (dots).

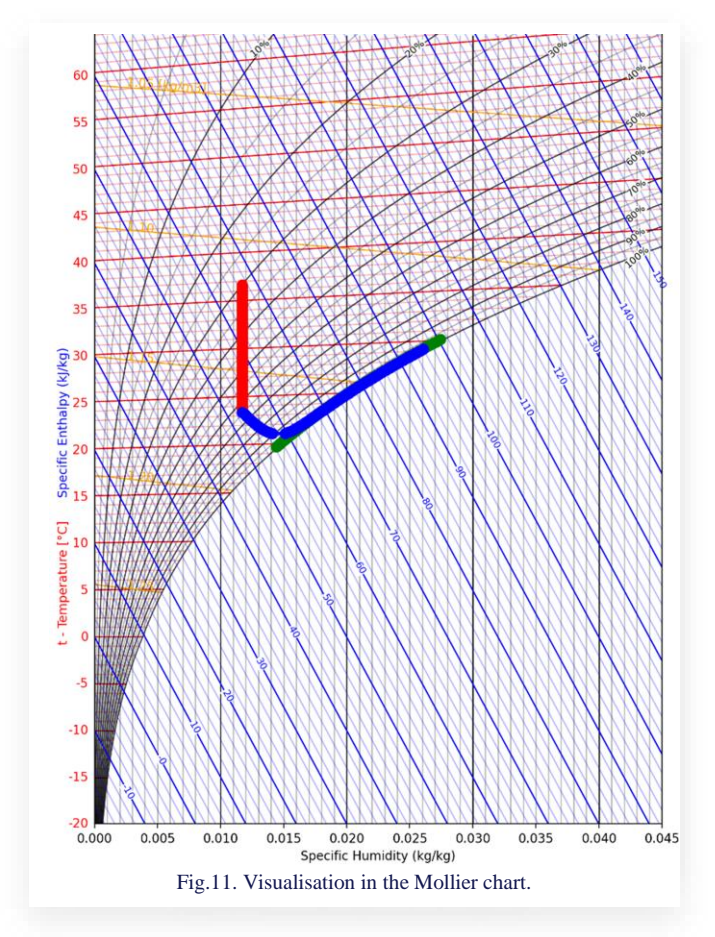


During the development and testing of the model, it was found that the model is very sensitive to values of heat and mass transfer coefficient, so for each simulation, the values of these coefficients were carefully checked. The current model provides a steady solution with constant heat and mass transfer coefficients. Below are listed values for test case 9:

- $h_m = 0.0224 \text{ m/s}$ mass transfer,
- $h_w = 26.38 \text{ W/(m}^2 \text{ K})$ wet channel heat transfer coef.,
- $h_d = 30.69 \text{ W/(m}^2 \text{ K)} \text{dry channel heat transfer coef.}$
- $U = 28.42 \text{ W/(m}^2 \text{ K)} \text{dry/water film heat transfer coef.}$

These are fundamental parameters characterising HMX and it is important to correctly calculate their values, because the model is very sensitive to them. An illustrative calculation of U by Eq. (7) for test case 9 is provided below:

 $U = 1/(1/30.69 + 0.0002/0.125 + 0.00015/0.15) = 28.42 \text{ W/(m}^2\text{ K)},$ $U \approx 1/(0.0326 + 0.0016 + 0.001).$



The overall heat transfer coefficient U is given by the reciprocal of the sum of individual thermal resistances (m² K/W): convection in the dry channel $1/h_d = 0.0326$, wicked paper $\delta_{pd}/k_{pa} = 0.0016$ and plastic plate $\delta_{pl}/k_{pl} = 0.001$. The last two resistances are constant and negligible; thus, the convection term is essential to adjust the M-cycle model. Another important parameter influencing the M-cycle effectiveness, apart from the inlet air temperature and humidity, is the mass flow rate in the dry and wet channels—particularly the ratio between them. This ratio is determined by the mass flow of the produced air at the dry channel outlet, which is subsequently used for cooling.

4. Conclusions

In the paper, the issues of sustainable AC were discussed related to population growth and ongoing climate change. The promising cooling technology from this point of view could be evaporative cooling. EC, particularly in dry climates, provide a promising alternative to VCC by achieving the cooling close to the wet-bulb temperature or even below by the M-cycle. We aimed our research to find new concepts of EC by implementing innovative materials, structures and ideas considering also literature sources mentioned in the introduction.

The main part of the paper was devoted to the introduction of the Python-based 1D model for the basic analysis of the M-cycle, which has been developed in the frame of the project MEBioSys. It is a Python-based computational tool for calculating heat and mass transfer in M-cycles and related psychrometric calculations, which are powered by the CoolProp library. It uses a spatially discretised differential equation solver and psychrometric chart (including the Mollier chart). Currently, the solver is just steady-state, and the unsteady solver is still under development. For the initial verification of the 1D model with a steady-state solver, the data from Pakari's study were used as a reference. Simulations of 15 test cases were performed. Our 1D model provides reasonable results and accurately fits Pakari's 1D model and his experimental data, which means that the numerical scheme is valid and can be used and adjusted for our planned experimental investigations, which will be the next step.

Currently, the model is focused solely on IEC with the M-cycle. However, we plan to enhance and extend it based on new experimental data:

- At the AGH University (under the project supported by the program "Excellence initiative – research university") the first direct evaporation test case data were collected and evaluated (not presented in this study),
- At the BUT University (under the project MEBioSys) the physical model for indirect evaporation is under development and it is planned to conduct measurements on new designs of indirect evaporative cooling using HX or even HMX (M-cycle).

The new validation datasets will be measured in the climatic chamber at BUT to evaluate the EC system under a wide range of climatic conditions. The own experiments will have an advantage of avoiding some uncertainties in interpreting simulation or experimental data from the literature. These experimental tests will also aim to enhance evaporative cooling systems through the use of new materials and structures. Based on the collected data, it will then be possible to adjust the model for different configurations of the M-cycle or, more generally, DEC/IEC systems.

In the development of our custom-designed EC system, we primarily consider the use of rapid prototyping (3D printing) supported by this 1D model. This approach is in our opinion more time-efficient than conducting full 3D CFD simulations to explore new designs. After the selection of the proper design, it is reasonable to use advanced CFD simulations of multiphase flows to adjust the 3D printed model and make refinements to improve some technical details, which can be behind the distinction of a simple 1D model or even can be hard to identify by experiments.

It can be concluded that this paper presents a promising verification result of the developed Python-based 1D model sug-

gesting a potential application in the advanced design of sustainable cooling technologies, primarily for air conditioning.

Acknowledgements

The research was supported by the project "Mechanical Engineering of Biological and Bio-inspired Systems", funded as project No. CZ.02.01.01/00/22_008/0004634 by Programme Johannes Amos Comenius, call Excellent Research. The research was also supported by the program "Excellence initiative – research university" for the AGH University.

References

- [1] Worldometer. (2024). World Population by Year. https://www.worldometers.info/world-population-by-country/ [accessed 13 Dec. 2024].
- [2] United Nations, Department of Economic and Social Affairs, Population Division. (2022). World Population Prospects 2022: Demographic profiles – Global. https://population.un.org/wpp/Graphs/DemographicProfiles/Line/900 [accessed 13 Dec. 2024].
- [3] Copernicus Climate Change Service. (2024). Temperature. Copernicus Climate Change Service. https://climate.copernicus.eu/climate-indicators/temperature [accessed 13 Dec. 2024].
- [4] IPCC (2018): Global Warming of 1.5°C. [Masson-Delmotte, V., Zhai, P., Pörtner, H.-O., Roberts, D., Skea, J., Shukla, P.R., Pirani, A., Moufouma-Okia, W., Péan, C., Pidcock, R., Connors, S., Matthews, J.B.R., Chen, Y., Zhou, X., Gomis, M.I., Lonnoy, E., Maycock, T., Tignor, M., & Waterfield, T. (eds.)]. An IPCC Special Report on the impacts of global warming of 1.5°C above preindustrial levels and related global greenhouse gas emission pathways, in the context of strengthening the global response to the threat of climate change, sustainable development, and efforts to eradicate poverty. Cambridge University Press, Cambridge, UK and New York, USA, 616. doi: 10.1017/9781009157940. https://www.ipcc.ch/site/assets/uploads/sites/2/2018/12/SR15_FAQ_Low_Res.pdf [accessed 13 Dec. 2024].
- [5] Copernicus Climate Change Service. (2024). *Copernicus:* 2024 *virtually certain to be the warmest year and first year above* 1.5°C. https://climate.copernicus.eu/copernicus-2024-virtually-certain-be-warmest-year-and-first-year-above-15degc [accessed 18 Dec. 2024].
- [6] Eyring, V., Bony, S., Meehl, G.A., Senior, C.A., Stevens, B., Stouffer, R.J., & Taylor, K.E. (2016). Overview of the Coupled Model Intercomparison Project Phase 6 (CMIP6) experimental design and organization, *Geoscientific Model Development*, 9(5), 1937–1958, https://doi.org/10.5194/gmd-9-1937-2016. https://gmd.copernicus.org/articles/9/1937/2016/ [accessed 13 Dec. 2024].
- [7] Pezzutto, S., Novelli, A., Zambito, A., Quaglini, G., Miraglio, P., Belleri, A., Bottecchia, L., Gantioler, S., Moser, D., Riviere, P., Etienne, A., Stabat, P., Berthou, T., Kranzl, L., Mascherbauer, P., Fallahnejad, M., Viegand, J., Jensen, C., Hummel, M., & Müller, A. (2022). Cooling technologies overview and market shares. Part 1 of the study "Renewable cooling under the revised Renewable Energy Directive ENER/C1/2018-493". (D. G. for European Commission, Ed.). Publications Office of the European Union. doi: 10.2833/799633
- [8] ASA. (2024). May Blue Marble Next Generation. Visible Earth. https://visibleearth.nasa.gov/images/74042/may-blue-marble-next-generation/740441 [accessed 13 Dec. 2024].

- [9] Acma, B., & Özyakali, N. (2020). Correlation Analysis of European Socioeconomic and Waste Management Structure Pursuant To EU-27 Waste Data 2018. *Theoretical and Applied Issues of Economics*, 191–204. doi: 10.17721/tppe.2020.41.7
- [10] Duan, Z., Zhan, C., Zhang, X., Mustafa, M., Zhao, X., Alimohammadisagvand, B., & Hasan, A. (2012). Indirect evaporative cooling: Past, present and future potentials. *Renewable and Sustainable Energy Reviews*, 16(9), 6823–6850. doi: 10.1016/j.rser. 2012.07.007
- [11] Tariq, R., Caliskan, H., & Sheikh, N.A. (2023). Maisotsenko Cycle for Heat Recovery in Gas Turbines: A Fundamental Thermodynamic Assessment. *Global Challenges*, 7(11), 2300178. doi: 10.1002/gch2.202300178
- [12] Gillan, L.E., Gillan, A.D., Kozlov, A., & Kalensky, D.C. (2011). An advanced evaporative condenser through the Maisotsenko cycle. *International Journal of Energy for a Clean Environment*, 12 (2-4), 251–258. doi: 10.1615/InterJEnerCleanEnv.2013006619
- [13] Pakari, A., & Ghani, S. (2019). Comparison of 1D and 3D heat and mass transfer models of a counter flow dew point evaporative cooling system: Numerical and experimental study. *International Journal of Refrigeration*, 99, 114–125. doi: 10.1016/j.ijrefrig. 2019.01.013
- [14] Amer, O., Boukhanouf, R., & Ibrahim, H.G. (2015). A Review of Evaporative Cooling Technologies. *International Journal of Environmental Science and Development*, 6(2), 111–117. doi: 10. 7763/ijesd.2015.V6.571
- [15] Prieto, A., Knaack, U., Auer, T., & Klein, T. (2019). COOL-FACADE: State-of-the-art review and evaluation of solar cooling technologies on their potential for façade integration. *Renewable and Sustainable Energy Reviews*, 101, 395–414. doi: 10.1016/j. rser.2018.11.015
- [16] Mahmood, M.H., Sultan, M., Miyazaki, T., Koyama, S., & Maisotsenko, V.S. (2016). Overview of the Maisotsenko cycle A way towards dew point evaporative cooling. *Renewable and Sustainable Energy Reviews*, 66, 537–555. doi: 10.1016/j.rser.2016. 08 022
- [17] Costelloe, B., & Finn, D. (2003). Indirect evaporative cooling potential in air—water systems in temperate climates. *Energy and Buildings*, 35(6), 573–591. doi: 10.1016/S0378-7788(02)00161-5
- [18] Kapilan, N., Isloor, A.M., & Karinka, S. (2023). A comprehensive review on evaporative cooling systems. *Results in Engineering*, 18, 101059. doi: 10.1016/j.rineng.2023.101059
- [19] Pescod, D. (1979). Heat exchanger for energy saving in an air-conditioning plant. *ASHRAE Transactions*, 85(2), 238 251.
- [20] Jradi, M., & Riffat, S. (2014). Experimental and numerical investigation of a dew-point cooling system for thermal comfort in buildings. *Applied Energy*, 132, 524–535. doi: 10.1016/j.apenergy.2014.07.040
- [21] Nawaz, K., Schmidt, S.J., & Jacobi, A.M. (2016). Adsorption and Desorption Isotherms Of Desiccants for Dehumidification Applications: Silica Aerogels and Silica Aerogel Coatings on Metal Foams. 15th International Refrigeration and Air Conditioning Conference at Purdue, July 14–17, 2016. http://Docs.Lib.Purdue.Edu/Iracc/1600 [accessed 13 Dec. 2024].
- [22] Mumtaz, M., Pamintuan, B.C., Fix, A.J., Braun, J.E., & Warsinger, D.M. (2023). Hybrid membrane dehumidification and dewpoint evaporative cooling for sustainable air conditioning. *Energy Conversion and Management*, 294. doi: 10.1016/j.enconman.2023.117547
- [23] Fix, A.J., Braun, J.E., & Warsinger, D.M. (2024). A general effectiveness-NTU modeling framework for membrane dehumidification systems. *Applied Thermal Engineering*, 236, 121514. doi: 10.1016/j.applthermaleng.2023.121514

- [24] Kumar, A., & Yadav, A. (2016). Experimental investigation of solar driven desiccant air conditioning system based on silica gel coated heat exchanger. *International Journal of Refrigeration*, 69. doi: 10.1016/j.ijrefrig.2016.05.008
- [25] Liu, L., Zeng, T., Huang, H., Kubota, M., Kobayashi, N., He, Z., Li, J., Deng, L., Li, X., Feng, Y., & Yan, K. (2020). Numerical modelling and parametric study of an air-cooled desiccant coated cross-flow heat exchanger. *Applied Thermal Engineering*, 169, 114901. doi: 10.1016/j.applthermaleng.2020.114901
- [26] Pan, Q.W., Xu, J., Wang, R.Z., & Ge, T.S. (2023). Analysis on desiccant coated heat exchangers based on a new performance parameter and thermodynamic model. *Applied Thermal Engineering*, 222, 119943. doi: 10.1016/j.applthermaleng.2022. 119943
- [27] Tu, Y.D., Wang, R.Z, Hua, L.J, Ge, T.S, & Cao, B.Y. (2017). Desiccant-coated water-sorbing heat exchanger: Weakly-coupled heat and mass transfer. *International Journal of Heat and Mass Transfer*, 113. doi: 10.1016/j.ijheatmasstransfer.2017.05.047
- [28] Abdulateef, J.M., Sopian, K., Alghoul, M.A., & Sulaiman, M.Y. (2009). Review on solar-driven ejector refrigeration technologies. *Renewable and Sustainable Energy Reviews*, 13(6–7), 1338–1349. doi: 10.1016/j.rser.2008.08.012
- [29] Ge T.S., Dai, Y.J., & Wang, R.Z. (2014). Review on solar powered rotary desiccant wheel cooling system. *Renewable and Sustainable Energy Reviews*, 39, 476–497. doi: 10.1016/j.rser. 2014.07.121
- [30] Pacak, A., & Worek, W. (2021). Review of Dew Point vaporative Cooling Technology for Air Conditioning Applications. *Applied Sciences*, 11(3). doi: 10.3390/app11030934
- [31] Pandelidis, D., & Anisimov, S. (2016). *Mathematical Modeling of the M-Cycle Heat and Mass Exchanger Used in Air Conditioning Systems*. Ph.D. Thesis, Wrocław University of Science and Technology, Wrocław, Poland.
- [32] Yan, M., He, S., Gao, M., Xu, M., Miao, J., Huang, X., & Hooman, K. (2021). Comparative study on the cooling performance of evaporative cooling systems using seawater and freshwater. *International Journal of Refrigeration*, 121, 23–32. doi: 10.1016/j.ijrefrig.2020.10.003
- [33] McDonald, K., & Sun, D.W. (2000). Vacuum cooling technology for the food processing industry: a review. *Journal of Food Engineering*, 45(2), 55–65. doi: 10.1016/S0260-8774(00)00041-8
- [34] Lim, H., Choi, S., Cho, Y., Kim, S., & Kim, M. (2020). Comparative thermodynamic analysis of membrane-based vacuum air dehumidification systems. *Applied Thermal Engineering*, 179, 115676. doi: 10.1016/j.applthermaleng.2020.115676
- [35] Yan, W., Yang, C., Liu, Y., Zhang, Y., Liu, Y., Cui, X., Meng, X., & Jin, L. (2024). A design optimization framework for vacuum-assisted hollow fiber membrane integrated evaporative water coolers. *Renewable Energy*, 230, 120848. doi: 10.1016/j. renene.2024.120848
- [36] Madejski, P., & Kuś, T. (2024). Evaporative Cooling: Lab Manual. Katedra Systemów Energetycznych i Urządzeń Ochrony Środowiska, AGH WIMiR (in Polish).
- [37] Shi, W., Ma, X., Min, Y., & Yang, H. (2024). Feasibility Analysis of Indirect Evaporative Cooling System Assisted by Liquid Desiccant for Data Centers in Hot-Humid Regions. *Sustainability*, 16(5). doi: 10.3390/su16052011
- [38] Gorshkov, V. (2013). Systems based on Maisotsenko cycle: Coolerado coolers. Bachelor's Thesis. Building services Engineering. December 2012. Mikkelin ammattikorkeakoulu. Mikkeli University of Applied Sciences.
- [39] Robichaud, R. (2007). Coolerado Cooler Helps to Save Cooling Energy and Dollars: New Cooling Technology Targets Peak

- Load Reduction. Technical Report, National Renewable Energy Lab. (NREL), Golden, CO, United States. doi: 10.2172/908968
- [40] Worek, W., Khinkis, M., Kalensky, D., & Maisotsenko, V. (2012). Integrated Desiccant–Indirect Evaporative Cooling System Utilizing the Maisotsenko Cycle. Conference Proceeding. ASME 2012 Heat Transfer Summer Conference collocated with the ASME 2012 Fluids Engineering Division Summer Meeting and the ASME 2012 10th International Conference on Nanochannels, Microchannels, and Minichannels, July 8–12, Rio Grande, Puerto Rico, USA. doi: 10.1115/HT2012-58039
- [41] Pandelidis, D., Niemierka, E., Pacak, A., Jadwiszczak, P., Cichon, A., Drag, P., Worek, W., & Cetin, S. (2020). Performance study of a novel dew point evaporative cooler in the climate of central Europe using building simulation tools. *Building* and Environment, 181, 107101. doi: 10.1016/j.buildenv.2020. 107101
- [42] Inobeme, A., Adetunji, C., Maliki, M., Eziukwu, C., Ngonso, B., Akhor, S., Ogundolie, F., & Dauda, W. (2023). Evaporative coolers for the postharvest management of fruits and vegetables. In Evaporative coolers for the postharvest management of fruits and vegetables (pp. 287–291). Elsevier. doi: 10.1016/B978-0-323-89864-5.00023-0
- [43] Rogdakis, E, & Tertipis, D. (2015). Maisotsenko cycle: technology overview and energy-saving potential in cooling systems. *Energy and Emission Control Technologies*, 3, 15–22. doi: 10.2147/eect.S62995
- [44] Xiao, X., & Liu, J. (2024). A state-of-art review of dew point evaporative cooling technology and integrated applications. *Renewable and Sustainable Energy Reviews*, 191, 114142. doi: 10.1016/j.rser.2023.114142
- [45] Taler, J., Jagieła, B., & Jaremkiewicz, M. (2022). Overview of the M-Cycle Technology for Air Conditioning and Cooling Applications. *Energies*, 15(5). doi: 10.3390/en15051814
- [46] Kang, H., Han, U., Lim, H., Lee, H., & Hwang, Y. (2021). Numerical investigation and design optimization of a novel polymer heat exchanger with ogive sinusoidal wavy tube. *International Journal of Heat and Mass Transfer*, 166, 120785. doi: 10.1016/j.ijheatmasstransfer.2020.120785
- [47] Kaur, I., & Singh, P. (2021). Critical evaluation of additively manufactured metal lattices for viability in advanced heat exchangers. *International Journal of Heat and Mass Transfer*, 168, 120858. doi: 10.1016/j.ijheatmasstransfer.2020.120858
- [48] Ma, X., Shi, W., Lu, L., & Yang, H. (2024). Performance assessment and optimization of water spray strategy for indirect evaporative cooler based on artificial neural network modeling and genetic algorithm. *Applied Energy*, 368, 123438. doi: 10.1016/j. apenergy.2024.123438
- [49] Ma, X., Shi, W., & Yang, H. (2022). Study on water spraying distribution to improve the energy recovery performance of indirect evaporative coolers with nozzle arrangement optimization. *Applied Energy*, 318. doi: 10.1016/j.apenergy.2022.119212
- [50] Wen, T., & Lu, L. (2019). Numerical and experimental study on internally cooled liquid desiccant dehumidification concerning film shrinkage shape and vapor condensation. *International Journal of Thermal Sciences*, 136, 316–327. doi: 10.1016/j.ijthermalsci.2018.10.046
- [51] Zhou, B., Lv, J., Zhu, M., Wang, L., Li, S., & Hu, E. (2024). Experiment for the performance of a thin membrane inclined automatic wicking dew-point evaporative cooling device based on simulation results. *Energy and Buildings*, 308, 114021. doi: 10.1016/j.enbuild.2024.114021
- [52] Press, W.H., Teukolsky, S.A., Vetterling, W.T., & Flannery, B.P. (2007). *Numerical Recipes: The Art of Scientific Computing* (3rd ed.). Cambridge University Press. New York, USA